FEBS Letters

FEBS PRESS science publishing by scientists

COMMUNICATION

Small molecule 3PO inhibits glycolysis but does not bind to 6-phosphofructo-2-kinase/fructose-2,6-bisphosphatase-3 (PFKFB3)

Besa Emini Veseli[1], Paola Perrotta[1], Pieter Van Wielendaele[2], Anne-Marie Lambeir[2], Anahita Abdali[3], Stefano Bellosta[3], Giovanni Monaco[4,5], Geert Bultynck[4], Wim Martinet[1] and Guido R. Y. De Meyer[1]

1 Laboratory of Physiopharmacology, University of Antwerp, Belgium
2 Laboratory of Medical Biochemistry, University of Antwerp, Belgium
3 Department of Pharmacological and Biomolecular Sciences, University of Milan, Italy
4 Laboratory of Molecular and Cellular Signalling, KU Leuven, Belgium
5 Australian Centre for Blood Diseases, Central Clinical School, Monash University, Melbourne, Australia

Correspondence
Guido R. Y. De Meyer, Laboratory of Physiopharmacology, University of Antwerp, Belgium
Tel: +32 3 265 27 37
E-mail: guido.demeyer@uantwerpen.be

Besa Emini Veseli and Paola Perrotta contributed equally to this work.

(Received 1 May 2020, revised 16 June 2020, accepted 26 June 2020)

doi:10.1002/1873-3468.13878

Edited by Michael Bubb

6-Phosphofructo-2-kinase/fructose-2,6-bisphosphatase isoform 3 (PFKFB3) is a key enzyme of the glycolytic pathway, and it plays an essential role in angiogenesis. 3-(3-Pyridinyl)-1-(4-pyridinyl)-2-propen-1-one (3PO) is frequently used as a glycolysis inhibitor and is thought to inhibit PFKFB3. However, this latter effect of 3PO has never been investigated in detail and was the aim of the present study. To demonstrate binding of 3PO to PFKFB3, we used isothermal titration calorimetry. However, 3PO did not bind to PFKFB3, even up to 750 μM, in contrast to 3 μM of AZ67, which is a potent and specific PFKFB3 inhibitor. Instead, 3PO accumulated lactic acid inside the cells, leading to a decrease in the intracellular pH and an inhibition of enzymatic reactions of the glycolytic pathway.

Keywords: 3PO; glycolysis; intracellular pH; isothermal titration calorimetry; PFKFB3

Glycolysis is an essential bioenergetic pathway in endothelial cells (ECs) generating up to 85% of total cellular ATP. A key regulating enzyme in the glycolytic pathway is 6-phosphofructo-2-kinase/fructose-2,6-bisphosphatase (PFKFB), which is involved in both synthesis and degradation of fructose-2,6-bisphosphate. Among the four known PFKFB isoforms, only PFKFB isoform 3 (PFKFB3) reveals a kinase-to-phosphatase ratio of about 740 : 1, which favors the formation of intracellular fructose-2,6-bisphosphate (Fru-2,6-P_2) and enhanced glycolysis [1,2]. Interestingly, the expression of PFKFB3 is upregulated in response to hypoxia and inflammatory stimuli [3,4]. Because silencing or inactivation of PFKFB3 reduces glycolysis and impairs vessel sprouting [5], PFKFB3 has become an attractive therapeutic target in preventing pathological angiogenesis. 3-(3-Pyridinyl)-1-(4-pyridinyl)-2-propen-1-one (3PO) has been reported as a novel compound that reduces glycolytic flux through competitive inhibition of PFKFB3 [6]. It causes a rapid reduction in

Abbreviations
3PO, 3-(3-Pyridinyl)-1-(4-pyridinyl)-2-propen-1-one; CHC, 2-Cyano-3-(4-hydroxyphenyl)-2-propenoic acid; DMEM, Dulbecco's Modified Eagle's medium; ECAR, extracellular acidification rate (ECAR); ECs, endothelial cells; Fru-2,6-P_2, fructose-2,6-bisphosphate; HUVECs, human umbilical vein endothelial cells; ITC, Isothermal titration calorimetry; MCTs, monocarboxylate transporters; NEAA, nonessential amino acids; PFK-1, phosphofructokinase-1; PFKFB, 6-phosphofructo-2-kinase/fructose-2,6-bisphosphatase; PFKFB3, 6-phosphofructo-2-kinase/fructose-2,6-bisphosphatase isoform 3; pHi, intracellular pH; VEGF, vascular endothelial growth factor.

Fru-2,6-P_2 levels and inhibits tumorigenic growth *in vivo*. It also diminishes ^{18}F-2-DG uptake within xenografts [6] and inhibits EC proliferation and migration, resulting in reduced vessel sprouting in EC spheroids, zebrafish embryos, and the postnatal mouse retina. Notably, all these effects of 3PO are attributable to only partial and transient inhibition of glycolysis [7].

Although 3PO and the more potent analogue PFK15 are considered to act as PFKFB3 inhibitors [8–12], thorough experimental evidence is currently lacking. Moreover, recent data indicate that 3PO is inactive in a PFKFB3 kinase assay (IC_{50} > 100 μM) and no crystal structure is available confirming binding of 3PO to PFKFB3 kinase [13]. It should be noted that 3PO does not inhibit the enzymatic activity of other enzymes involved in the glycolytic pathway such as hexokinase, glucose-6-phosphate dehydrogenase, transketolase, phosphofructokinase, pyruvate kinase, and lactate dehydrogenase [7]. In the present study, we demonstrate that the antiglycolytic activity of 3PO relies on its ability to interfere with intracellular milieu acidification, rather than on a direct binding to PFKFB3.

Materials and methods

Glycolysis measurements

Glycolysis was measured *in vitro* using a Glycolysis Cell-Based Assay Kit (Cayman Chemical, Ann Arbor, MI, USA) following the manufacturer's instructions. Briefly, human umbilical vein ECs (HUVECs) were seeded in a 96-well culture plate at a density of 15 000 cells per well and incubated overnight at 37 °C in M199 culture medium, supplemented with 0.25% heat-inactivated FBS, 1% nonessential amino acids (NEAA), and antibiotics. Thereafter, cells were treated with 3PO (Sigma-Aldrich, Saint Louis, MO, USA; 2–100 μM) for 24 h and assayed to determine the L-lactate concentration in the culture medium. A neutral red viability assay was performed as described [14] to test cell viability.

Glycolytic flux was also assessed in HUVECs by measuring the extracellular acidification rate (ECAR) using a Seahorse XFp Analyzer (Agilent Technologies, Santa Clara, CA, USA) and following manufacturer recommended protocol. ECAR values were expressed in units of mpH·min^{-1}, which follow the changes in pH in the media surrounding the cells, an acidification mostly due to glycolytic proton efflux [15]. Assays were performed prior to experiments to determine optimal cell seeding density, viability, and optimal concentrations of each compound. Briefly, 10 000 HUVECs per well were plated into XF8 polystyrene cell culture plates. After 16 h of incubation at 37 °C, cells were treated with 3PO (0, 20 or 40 μM) for 5 h. Prior to performing a glycolysis stress test, growth medium in the wells of XF cell plates was exchanged with the appropriate Seahorse assay medium (Agilent Technologies, 103335-100). Baseline rates were measured three times prior to any injection. Firstly, glucose (Sigma-Aldrich, G8270; 10 mM final concentration) was injected into the medium to provide a measure of glycolytic rate. Subsequently, oligomycin, a mitochondrial ATP synthase inhibitor (Sigma-Aldrich, 75351; 2 μM final concentration) was injected, blocking oxidative phosphorylation and giving an estimate of glycolytic capacity. Finally, 2-DG (Sigma-Aldrich, D8375; 50 mM final concentration) was injected, which is a glucose analog that inhibits glycolysis, providing an estimate of nonglycolytic acidification. All compounds were prepared in assay medium and adjusted to pH 7.4. Glycolytic capacity was calculated as the difference between ECAR following the injection of 2 μM oligomycin and the basal ECAR reading [16].

Intracellular lactate measurements

Intracellular lactate levels were measured *in vitro* using an L-Lactate Assay Kit (Cayman Chemical) according to the manufacturer's protocol. HUVECs were plated into a cell culture plate until 80% confluency in M199 growth medium supplemented with 20% FBS, 1% NEAA, and antibiotics. Next, HUVECs were treated with 3PO (20 μM) or vehicle (DMSO) for 24 h. A cell count was performed with an automated cell counter (Countess® II FL; Life Technologies, Carlsbad, CA, USA). After deproteinization with 0.25 M metaphosphoric acid, potassium carbonate (5 M) was added to the cell pellet to neutralize the acid. Following centrifugation (10 000 ***g*** for 5 min) at 4 °C, the supernatant was used for assaying. Lactate fluorescent substrate was used as a fluorophore while fluorescence (λ_{ex} = 540 nm; λ_{em} = 595 nm) was measured and normalized to the cell number. 2-Cyano-3-(4-hydroxyphenyl)-2-propenoic acid (CHC), a classical inhibitor of monocarboxylate transporters (MCTs), was used as a reference compound.

Intracellular pH assay

Intracellular pH (pHi) changes were measured with a Fluorometric pHi Assay Kit (Sigma-Aldrich, MAK150) following the manufacturer's protocol. In brief, HUVECs were plated overnight in M199 growth medium supplemented with 20% FBS, 1% NEAA, and antibiotics in a 96-well culture plate. Subsequently, the fluorescent pH indicator BCFL-AM was added for 30 min. 3PO (20 μM) was diluted in Hank's Buffer (HBSS) containing 20 mM HEPES and added to the cells. Fluorescence (λ_{ex} = 490 nm;

λ_{em} = 535 nm) was measured 5 h after addition of 3PO. CHC, a well-known inhibitor of MCTs, was used as a reference compound.

In vitro angiogenesis assay

Inhibition of endothelial tube formation by 3PO was monitored using an *in vitro* angiogenesis assay kit (Millipore, Burlington, MA, USA) following the manufacturer's instructions. Briefly, HUVECs were cultured in M199 medium supplemented with 20% FBS, 1% NEAA, and antibiotics. After addition of 3PO (0–20 μM) for 16 h, changes in tube formation and formation of cellular networks were evaluated. Capillary tube branching points were counted in five random fields per concentration.

Endothelial cell migration assay

Murine immortalized heart ECs (H5V) were cultured on 12-well plates in Dulbecco's Modified Eagle's medium (DMEM) medium supplemented with 10% FBS and antibiotics. After reaching confluence, H5V were starved overnight in DMEM containing 0.5% FBS. Each well was marked below the plate surface by drawing a vertical line. Five different scratches intercepting the marked line were done in each well using a 200-μL sterile tip. Pictures of scratches were taken before and after 18 h of incubation with DMEM (with 2.5% FBS) with or without 3PO (20 μM) and with or without vascular endothelial growth factor (VEGF, 10 ng·mL^{-1}). Next, the mean closure of five different scratches was analyzed using IMAGEJ software (National Institutes of Health, Bethesda, MD, USA). EC migration was expressed as the percentage of scratch closure after 18 h vs the initial area by using the following formula: % closure = [(scratched area at 0 h − scratched area at 18 h)/scratched area at 0 h] × 100.

Aortic sprouting

An aortic ring assay was performed as previously described [17]. In brief, murine thoracic aortas were dissected, cleaned under sterile conditions, transferred to 10-cm culture dishes, and cut into 0.5-mm thick rings with a sterile scalpel. After overnight starvation in serum-free Opti-MEM at 37 °C, ring segments were transferred into wells of a 96-well plate coated with 50 μL of a freshly prepared collagen type I solution (1 mg·mL^{-1}). The aortic rings remained in Opti-MEM (supplemented with 2.5% FBS and antibiotics) in the presence or absence of 3PO and/or VEGF (50 ng·mL^{-1}; R&D Systems, Minneapolis, MN, USA). Medium was replaced every 2 days. On day 6, rings were fixed with 4% paraformaldehyde, stained with von Willebrand factor antibody (anti-vWF, PC054, Binding Site) and DAPI prior to fluorescence microscopy imaging. The number of sprouts was counted for each ring, and sprout numbers per ring were averaged for each group and graphed.

Isothermal titration calorimetry

Binding of 3PO and AZ PFKFB3 67 (further abbreviated as AZ67, Tocris, used as control) to PFKFB3 was analyzed by calorimetry using a MicroCal Peaq-ITC isothermal titration calorimeter (nonautomated version; Malvern Panalytical, Malvern, UK). Prior to ITC analysis, recombinant human PFKFB3 from *Escherichia coli* [Flemish Institute for Biotechnology (VIB), Protein Service Facility, University of Ghent, Belgium] was dialyzed against 2 L buffer (40 mM Tris, 500 mM NaCl, 5 mM $MgCl_2$, 2 mM DTT at pH 7.4) for 2 h at 4 °C under constant stirring, followed by switching to a novel 2 L buffer vial and overnight dialysis. For this purpose, Slide-A-Lyzer Dialysis G2 cassettes (Thermo Fisher Scientific, Waltham, MA, USA) were used. The concentration of the sample after dialysis was determined through UV-absorbance at 280 nm using a SpectraMax Plus 384 (Molecular Devices, San Jose, CA, USA). A small portion of the second dialysis buffer volume was kept for matching the ligand solutions (AZ67 or 3PO). All buffers were prepared in ultrapure water (18.2 MΩ.cm), equilibrated to room temperature, and degassed for 15 min in an ultrasonication bath before use. All titrations were performed with the same PFKFB3 sample, diluted to a working concentration of 3 μM, and with the same titration conditions (except for the ligand concentration) in order to allow mutual comparison between the different runs.

The reference cell of the Peaq-ITC was filled with degassed ultrapure water. The PFKFB3 solution was put in the sample cell after a 2 min pre-equilibration with assay buffer (same recipe as dialysis buffer). The ligand solution was administered in the injection syringe. Titration conditions were as follows: One initial injection of 0.4 μL was followed by 14 injections of 2.5 μL. The initial spacing was set to 180 s, while the remaining spacing was set to 150 s. The sample cell was continuously stirred at 750 r.p.m. Temperature was set to 37 °C before loading and kept constant during the complete run. The DP (differential power between the reference and sample cells to maintain a zero temperature difference between the cells) was set to 5.

To determine the dilution heats for each PFKFB3-ligand concentration combination, control titrations were performed consisting of injection of ligand into the buffer-filled cell (thus in the absence of PFKFB3, without binding). Thermograms were analyzed using the MICROCAL PEAQ-ITC ANALYSIS software (Malvern Pananalytical), using the 'one set of sites' binding model, by including the corresponding control titration. In order to visually compare the different titrations with completely different molar ratios, the data were transformed to generated heat (ΔH) per injection.

Statistics

All data are expressed as mean ± SEM. Statistical analyses were performed using SPSS software (version 25; IBM, Armonk, NY, USA). Statistical tests are specified in the figure legends. *N* indicates the number of times an experiment has been repeated. Differences were considered significant at $P < 0.05$.

Results

3PO inhibits glycolysis in endothelial cells

Lactate measurements in the culture medium of HUVECs as well as Seahorse ECAR measurements showed that 3PO inhibits glycolysis in a concentration-dependent manner (Fig. 1A,B). The ECAR diminished by more than 50% after treatment with 20 μM 3PO (Fig. 1B). Viability of HUVECs was not affected when cells were treated with 3PO up to 20 μM (Fig. 1C). However, cytotoxic effects were noticed after exposure to higher 3PO concentrations (40 and 100 μM).

3PO inhibits capillary tube formation, EC migration, and formation of aortic sprouts

To confirm whether glycolysis inhibition by 3PO in ECs affects neoangiogenesis, an *in vitro* Matrigel assay with HUVECs was performed. This assay is based on the ability of ECs to form cord and mesh structures when seeded on a growth factor-enriched matrix. 3PO fully inhibited cord formation at 20 μM. At lower concentrations (5–10 μM), mesh structures consisting of EC chords were visible but their numbers were reduced in a concentration-dependent manner. A healthy network of chord structures was formed in the absence of 3PO (Fig. 2A). Branch point counting demonstrated an inverse correlation between the amount of branch points and the concentration of 3PO (Fig. 2B). Apart from inhibition of capillary tube formation, 3PO inhibited EC migration after scratching EC monolayers (Fig. 3) and prevented aortic sprouting (Fig. 4) both under basal conditions and after stimulation with VEGF.

3PO does not bind PFKFB3

Isothermal titration calorimeter measurements did not show any binding of 3PO toward recombinant PFKFB3. Even usage of 750 μM 3PO as final concentration did not yield any binding indication. In contrast, AZ67, which is a potent and specific PFKFB3 inhibitor [13] that was used as a positive control clearly showed binding toward recombinant PFKFB3 (Fig. 5A).

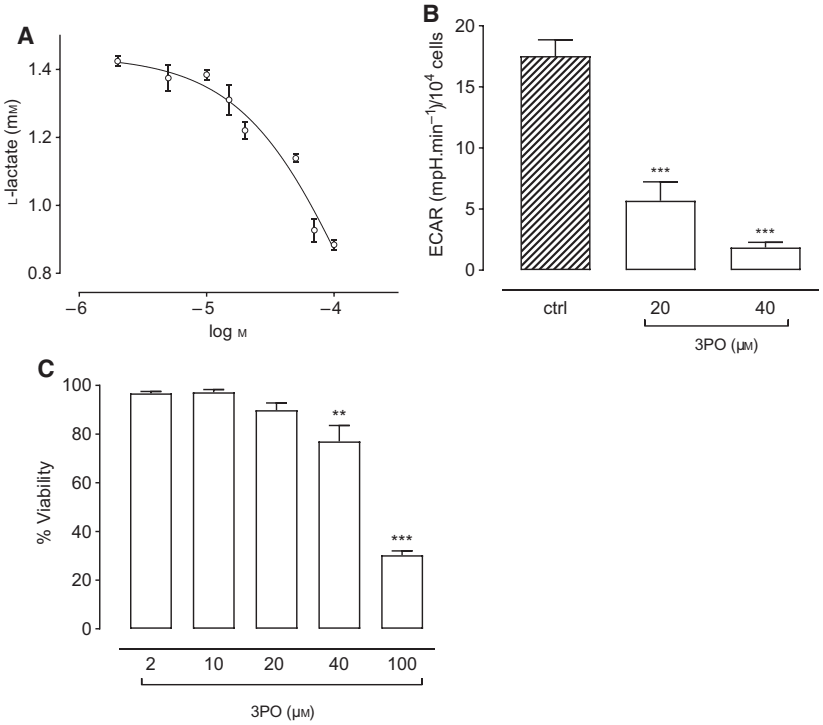

Fig. 1. 3PO inhibits glycolysis *in vitro*. (A) HUVECs were cultured and treated with 3PO (2–100 μM) for 24 h. Extracellular lactate was measured to evaluate glycolysis. (B) Glycolytic flux was assessed by measuring the ECAR using a Seahorse XFp Analyzer. Cultured HUVECs were treated without or with 3PO (20 or 40 μM) for 5 h. (C) 3PO (2, 10, 20 μM) did not show cytotoxic effects up to 24 h of treatment compared to vehicle (DMSO), whereas concentrations starting from 40 μM 3PO onward decreased cell viability. $^{**}P < 0.01$, $^{***}P < 0.001$ (one-way ANOVA followed by Dunnett test, $N = 3$).

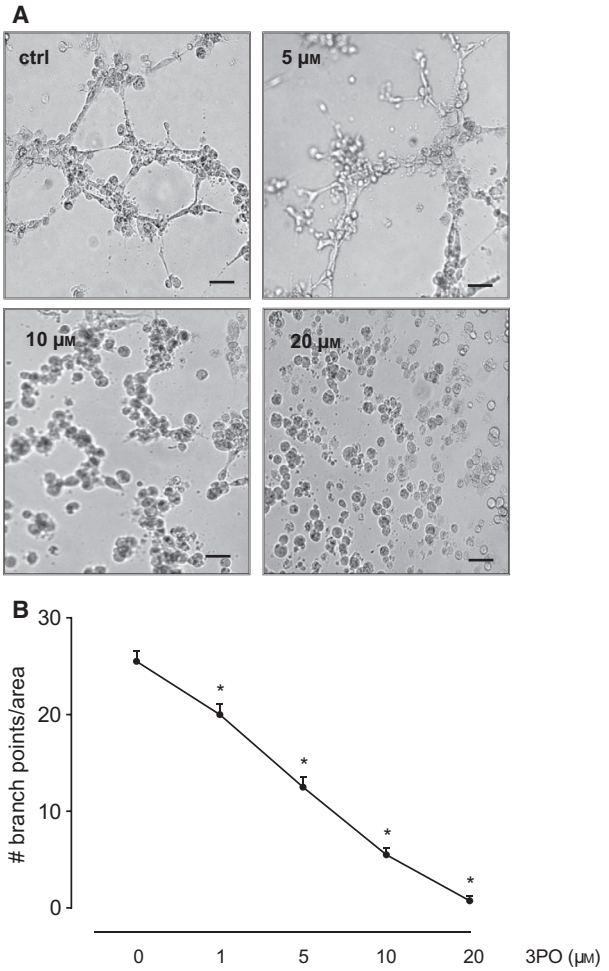

Fig. 2. 3PO inhibits EC tube formation. (A) Representative images of an *in vitro* angiogenesis assay. HUVECs were seeded on ECMatrix in the presence or absence of 3PO (5, 10, 20 μM) for 16 h. Images of tube formation and branching were taken and quantified. Scale bar = 100 μm. (B) The progression of angiogenesis was quantified by counting the amount of capillary tube branch points at different concentrations. $*P < 0.05$ vs control (Mann–Whitney *U*-test, $N = 4$).

3PO induces intracellular lactate accumulation and decreases the intracellular pH

Disruption of the pHi has been shown to play an important role in regulating angiogenesis [18] and glycolysis [18,19]. Therefore, we studied the effect of 3PO treatment on the pHi in ECs. 3PO (20 μM) induced intracellular acidification, as shown by a significant decrease in pHi in HUVECs (Fig. 5B). Given that lactate is an important regulator of pH [20], we measured intracellular lactate levels in HUVECs after treatment with 3PO and showed that it increased the lactate concentration intracellularly (Fig. 5C). CHC, a well-known inhibitor of MCTs [21], was used as a reference compound.

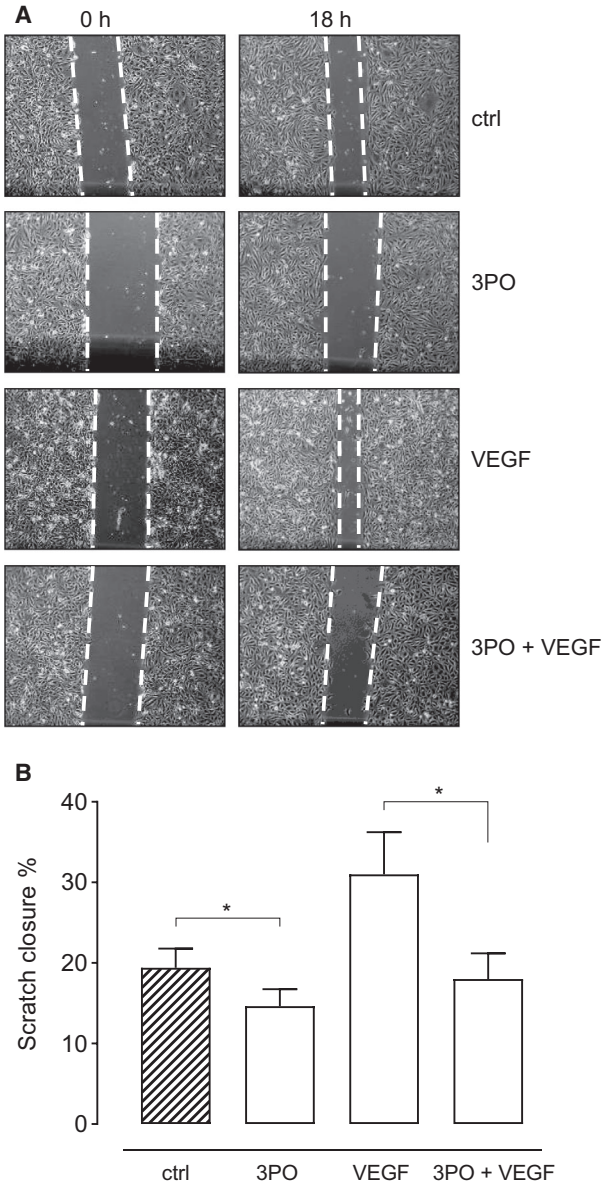

Fig. 3. 3PO inhibits EC migration. (A) Representative images of a scratch assay. Murine immortalized heart ECs (H5V) were starved, subsequently wounded, and treated with DMEM (2.5% FBS) with or without 20 μM 3PO, and with or without 10 ng·mL^{-1} VEGF for 18 h. (B) The wound area was measured at 0 and 18 h, and migration was quantified. Factorial ANOVA, $N = 5–7$; effect of 3PO: $P = 0.020$; effect of VEGF: $P = 0.046$; interaction: $P = 0.255$; $*P < 0.05$.

Discussion

The rate of glycolysis in ECs is much higher than in any other healthy cell type. Accordingly, the majority of ATP produced in these cells is through the anaerobic glycolytic pathway. These findings highlight glycolysis inhibition as a promising antiangiogenic strategy.

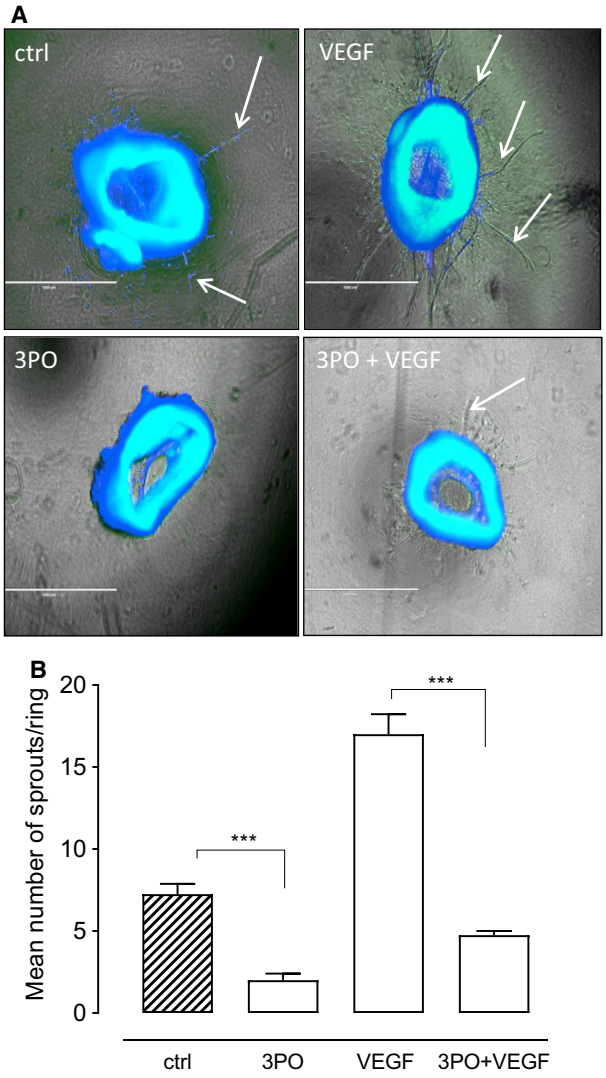

Fig. 4. 3PO inhibits aortic sprouting. (A) Aortic rings from ApoE$^{-/-}$ mice were embedded in collagen type I and treated with Opti-MEM (supplemented with 2.5% FBS) in the presence or absence of 20 μM 3PO and/or VEGF (50 ng·mL^{-1}) 2.5% (vol/vol) FBS or VEGF 50 ng·mL^{-1}. At day 6, rings were fixed and stained to delineate ECs. Images of ring sprouting were obtained and quantified. Scale bar = 1 mm. (B) Sprouts were quantified, $N = 4$ mice. ***$P < 0.001$ Factorial ANOVA, effect of 3PO: $P < 0.001$, effect of VEGF: $P < 0.001$, interaction: $P < 0.001$.

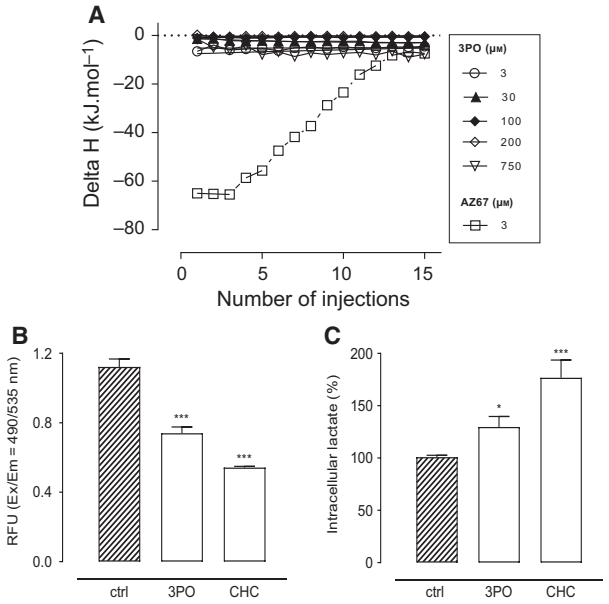

Fig. 5. Mechanism of glycolysis inhibition by 3PO. (A) 3PO does not bind to PFKFB3. Binding of 3PO to PFKFB3 was analyzed via calorimetry using a MicroCal ITC ITC. Discharged or absorbed heat during the eventual interaction between the PFKFB3 protein and 3PO (3–750 μM) was measured ((Δ*H*). PFKFB3 inhibitor AZ67 (3 μM) was used as a positive control. Indicated concentrations are the concentrations in the injection syringe of the Peaq-ITC, $N = 3$. (B) 3PO decreases the pHi. HUVECs were treated with 3PO (20 μM) for 5 h. Fluorescent pH indicator BCFL-AM was added, and fluorescence was measured. CHC (2 mM) was used as a positive control, $N = 6$–20. ***$P < 0.001$ vs control (one-way ANOVA followed by Dunnett test). (C) 3PO induces intracellular lactate accumulation. HUVECs were treated with 3PO (20 μM) for 24 h. Lactate fluorescent substrate was added, and fluorescence was measured, $N = 4$–9. *$P < 0.05$, ***$P < 0.001$ vs control (one-way ANOVA followed by Dunnett test).

Using computational techniques, 3PO was identified as a small-molecule inhibitor of PFKFB3 [6]. Follow-up experiments indicate that 3PO reduces Fru-2,6-P_2 levels and glycolytic flux [6]. Since then, administration of 3PO has been considered as an attractive therapeutic strategy in cancer research, acute lung injury, lung fibrosis, and atherosclerosis [22–25]. The ability of 3PO to inhibit glycolysis was confirmed in the present study. Indeed, by using Seahorse technology, we could demonstrate that 3PO inhibits glycolysis in a concentration-dependent manner in HUVECs, resulting in an up to 50% reduction in glycolytic rate. Moreover, 3PO inhibits capillary tube formation, migration of ECs, and formation of aortic sprouts, which are all processes that heavily depend on glycolysis. However, an enzyme binding assay via ITC did not reveal binding of 3PO to PFKFB3, not even when titrating with up to 750 μM final concentration, which is more than 35 times higher than the 20 μM 3PO used in the *in cellulo* experiments. This raises considerable doubts as to whether 3PO does work via PFKFB3 inhibition. Importantly, 3PO does not inhibit the enzymatic activity of other enzymes involved in the glycolytic pathway, such as hexokinase, glucose 6-phosphate dehydrogenase, transketolase, glyceraldehyde 3-

phosphate dehydrogenase, pyruvate kinase, and lactate dehydrogenase. The question remains which mechanism is responsible for the inhibition of glycolysis by 3PO. The present study shows that the inhibitory effect of 3PO on glycolysis relies on the ability of this compound to cause an imbalance in pHi by accumulating lactic acid inside the cell. It is known that some glycolytic enzymes including lactate dehydrogenase and phosphofructokinase-1 (PFK-1) are very pH sensitive. A change of less than one pH unit, even a few tenths, may reduce the activity of PFK-1 by more than 10-fold [18,19,26–28]. Moreover, PFKFB3, also known as PFK-2, has been shown to be allosterically regulated by hydrogen ion concentrations [29]. On the other hand, lactate is an important regulator of pH [20], and hence, the intracellular increase in this metabolite leads to intracellular milieu acidification, thus indirectly affecting the rate of glycolysis. Manipulating intracellular acidification has been considered to have therapeutic utility in tumors. One of the strategies includes the inhibition of MCTs. Among different acid extruders present in the cell membrane, MCTs 1 and 4 are responsible for bumping out lactate and hydrogen ions. More specifically, a multitude of studies has documented that MCT1 or MCT4 inhibition conferred antiangiogenic effects and block tumor growth [30–32]. In this light, we do not rule out the possibility that 3PO acts as an inhibitor of one or more MCT transporters.

Altogether, our study indicates that the inhibitory effect of 3PO on PFKFB3 enzymatic activity, glycolysis, and angiogenesis is not mediated through direct binding to the PFKFB3 protein, as already suggested previously [6]. This is the first study to report these findings, as no previous studies have investigated the thermodynamic profile and biomolecular interactions of 3PO and PFKFB3. Intracellular acidification and lactate accumulation are followed by a chain reaction starting with MCT1/4 inhibition, pHi decrease, influence of pH-dependent rate-limiting enzymes, and glycolysis suppression. This backward chain reaction supports our hypothesis of 3PO targeting MCT 1 and MCT 4. The identification of this target may have an important impact on angiogenesis research and on the development of specific antiangiogenic treatments, which has implications for a variety of pathologies.

Acknowledgements

This work was supported by the University of Antwerp (BOF, grant number 29068 and 40183). Besa Emini Veseli, Paola Perrotta, and Anahita Abdali are PhD fellows of the Horizon 2020 program of the European Union—Marie Skłodowska-Curie Actions, Innovative Training Networks (ITN), Call: H2020-MSCA-ITN-2015, NUMBER—675527—MOGLYNET. The authors are grateful to Dr. Bronwen Martin for critical reading of the manuscript.

Author contributions

GRYDM, WM, SB and A-ML conceived and designed the research; BEV, PP, PVW, AA and GM acquired the data; BEV, PP, AA, PVW, GM, SB, WM and GRYDM analyzed and interpreted the data; BEV, PP, AA and GRYDM performed statistical analysis; GRYDM, WM and SB handled funding and supervision; BEV, PP, WM and GRYDM drafted the manuscript; and PVW, A-ML, SB, GM, GB, WM and GRYDM made the critical revision of the manuscript for important intellectual content.

References

1 Yalcin A, Telang S, Clem B and Chesney J (2009) Regulation of glucose metabolism by 6-phosphofructo-2-kinase/fructose-2,6-bisphosphatases in cancer. *Exp Mol Pathol* **86**, 174–179.
2 Sakakibara R, Kato M, Okamura N, Nakagawa T, Komada Y, Tominaga N, Shimojo M and Fukasawa M (1997) Characterization of a human placental fructose-6-phosphate, 2-kinase/fructose-2,6-bisphosphatase. *J Biochem* **122**, 122–128.
3 Minchenko O, Opentanova I and Caro J (2003) Hypoxic regulation of the 6-phosphofructo-2-kinase/fructose-2,6-bisphosphatase gene family (PFKFB-1-4) expression *in vivo*. *FEBS Lett* **554**, 264–270.
4 Obach M, Navarro-Sabaté A, Caro J, Kong X, Duran J, Gómez M, Carlos Perales J, Ventura F, Luis Rosa J and Bartrons R (2004) 6-Phosphofructo-2-kinase (pfkfb3) gene promoter contains hypoxia-inducible factor-1 binding sites necessary for transactivation in response to hypoxia. *J Biol Chem* **279**, 53562–53570.
5 De Bock K, Georgiadou M, Schoors S, Kuchnio A, Wong BW, Cantelmo AR, Quaegebeur A, Ghesquière B, Cauwenberghs S, Eelen G *et al.* (2013) Role of PFKFB3-driven glycolysis in vessel sprouting. *Cell* **154**, 651–663.
6 Clem B, Telang S, Clem A, Yalcin A, Meier J, Simmons A, Rasku MA, Arumugam S, Dean WL, Eaton J *et al.* (2008) Small-molecule inhibition of 6-phosphofructo-2-kinase activity suppresses glycolytic flux and tumor growth. *Mol Cancer Ther* **7**, 110–120.
7 Schoors S, De Bock K, Cantelmo AR, Georgiadou M, Ghesquière B, Cauwenberghs S, Kuchnio A, Wong BW, Quaegebeur A, Goveia J *et al.* (2014) Partial and transient reduction of glycolysis by PFKFB3 blockade

reduces pathological angiogenesis. *Cell Metab* **19**, 37–48.
8 Rao TN, Hansen N, Hilfiker J, Rai S, Majewska J-M, Leković D, Gezer D, Andina N, Galli S, Cassel T *et al.* (2019) JAK2-mutant hematopoietic cells display metabolic alterations that can be targeted to treat myeloproliferative neoplasms. *Blood* **134**, 1832–1846.
9 Cao Y, Zhang X, Wang L, Yang Q, Ma Q, Xu J, Wang J, Kovacs L, Ayon RJ, Liu Z *et al.* (2019) PFKFB3-mediated endothelial glycolysis promotes pulmonary hypertension. *Proc Natl Acad Sci USA* **116**, 13394–13403.
10 Houddane A, Bultot L, Novellasdemunt L, Johanns M, Gueuning M-A, Vertommen D, Coulie PG, Bartrons R, Hue L and Rider MH (2017) Role of Akt/PKB and PFKFB isoenzymes in the control of glycolysis, cell proliferation and protein synthesis in mitogen-stimulated thymocytes. *Cell Signal* **34**, 23–37.
11 Pisarsky L, Bill R, Fagiani E, Dimeloe S, Goosen RW, Hagmann J, Hess C and Christofori G (2016) Targeting Metabolic symbiosis to overcome resistance to anti-angiogenic therapy. *Cell Rep* **15**, 1161–1174.
12 Finucane OM, Sugrue J, Rubio-Araiz A, Guillot-Sestier M-V and Lynch MA (2019) The NLRP3 inflammasome modulates glycolysis by increasing PFKFB3 in an IL-1beta-dependent manner in macrophages. *Sci Rep* **9**, 4034.
13 Boyd S, Brookfield JL, Critchlow SE, Cumming IA, Curtis NJ, Debreczeni J, Degorce SL, Donald C, Evans NJ, Groombridgeet S *et al.* (2015) Structure-based design of potent and selective inhibitors of the metabolic kinase PFKFB3. *J Med Chem* **58**, 3611–3625.
14 Repetto G, del Peso A and Zurita JL (2008) Neutral red uptake assay for the estimation of cell viability/cytotoxicity. *Nat Protoc* **3**, 1125–1131.
15 Zhang J, Nuebel E, Wisidagama DRR, Setoguchi K, Hong JS, Van Horn CM, Imam SS, Vergnes L, Malone CS, Koehler CM *et al.* (2012) Measuring energy metabolism in cultured cells, including human pluripotent stem cells and differentiated cells. *Nat Protoc* **7**, 1068–1085.
16 Divakaruni AS, Paradyse A, Ferrick DA, Murphy AN and Jastroch M (2014) Analysis and interpretation of microplate-based oxygen consumption and pH data. *Methods Enzymol* **547**, 309–354.
17 Baker M, Robinson SD, Lechertier T, Barber PR, Tavora B, D'Amico G, Jones DT, Vojnovic B and Hodivala-Dilke K. (2011) Use of the mouse aortic ring assay to study angiogenesis. *Nat Protoc* **7**, 89–104.
18 White KA, Grillo-Hill BK and Barber DL (2017) Cancer cell behaviors mediated by dysregulated pH dynamics at a glance. *J Cell Sci* **130**, 663–669.
19 Quach CH, Jung K-H, Lee JH, Park JW, Moon SH, Cho YS, Choe YS and Lee K-H (2016) Mild alkalization acutely triggers the warburg effect by enhancing hexokinase activity via voltage-dependent anion channel binding. *PLoS One* **11**, e0159529.
20 Huber V, Camisaschi C, Berzi A, Ferro S, Lugini L, Triulzi T, Tuccitto A, Tagliabue E, Castelli C and Rivoltini L (2017) Cancer acidity: an ultimate frontier of tumor immune escape and a novel target of immunomodulation. *Semin Cancer Biol* **43**, 74–89.
21 Sonveaux P, Végran F, Schroeder T, Wergin MC, Verrax J, Rabbani ZN, De Saedeleer CJ, Kennedy KM, Diepart C, Jordan BF *et al.* (2008) Targeting lactate-fueled respiration selectively kills hypoxic tumor cells in mice. *J Clin Invest* **118**, 3930–3942.
22 Conradi LC, Brajic A, Cantelmo AR, Bouché A, Kalucka J, Pircher A, Brüning U, Teuwen L-A, Vinckier S, Ghesquière B *et al.* (2017) Tumor vessel disintegration by maximum tolerable PFKFB3 blockade. *Angiogenesis* **20**, 599–613.
23 Gong Y, Lan H, Yu Z, Wang M, Wang S, Chen Y, Rao H, Li J, Sheng Z and Shao J (2017) Blockage of glycolysis by targeting PFKFB3 alleviates sepsis-related acute lung injury via suppressing inflammation and apoptosis of alveolar epithelial cells. *Biochem Biophys Res Commun* **491**, 522–529.
24 Xie N, Tan Z, Banerjee S, Cui H, Ge J, Liu R-M, Bernard K, Thannickal VJ and Liu G (2015) Glycolytic reprogramming in myofibroblast differentiation and lung fibrosis. *Am J Respir Crit Care Med* **192**, 1462–1474.
25 Perrotta P, Van der Veken B, Van Der Veken P, Pintelon I, Roosens L, Adriaenssens E, Timmerman V, Guns P-J, De Meyer GRY and Martinet W (2020) Partial inhibition of Glycolysis reduces atherogenesis independent of intraplaque neovascularization in mice. *Arterioscler Thromb Vasc Biol* **40**, 1168–1181.
26 Andres V, Carreras J and Cusso R (1990) Regulation of muscle phosphofructokinase by physiological concentrations of bisphosphorylated hexoses: effect of alkalinization. *Biochem Biophys Res Commun* **172**, 328–334.
27 Kamp G, Schmidt H, Stypa H, Feiden S, Mahling C and Wegener G (2007) Regulatory properties of 6-phosphofructokinase and control of glycolysis in boar spermatozoa. *Reproduction* **133**, 29–40.
28 Trivedi B and Danforth WH (1966) Effect of pH on the kinetics of frog muscle phosphofructokinase. *J Biol Chem* **241**, 4110–4112.
29 Putney LK and Barber DL (2004) Expression profile of genes regulated by activity of the Na-H exchanger NHE1. *BMC Genom* **5**, 46.
30 Hong CS, Graham NA, Gu W, Espindola Camacho C, Mah V, Maresh EL, Alavi M, Bagryanova L, Krotee PAL, Gardner BK *et al.* (2016) MCT1 modulates cancer cell pyruvate export and growth of tumors that co-express MCT1 and MCT4. *Cell Rep* **14**, 1590–1601.

31 Sonveaux P, Copetti T, De Saedeleer CJ, Végran F, Verrax J, Kennedy KM, Moon EJ, Dhup S, Danhier P, Frérart F *et al.* (2012) Targeting the lactate transporter MCT1 in endothelial cells inhibits lactate-induced HIF-1 activation and tumor angiogenesis. *PLoS One* **7**, e33418.

32 Voss DM, Spina R, Carter DL, Lim KS, Jeffery CJ and Bar EE (2017) Disruption of the monocarboxylate transporter-4-basigin interaction inhibits the hypoxic response, proliferation, and tumor progression. *Sci Rep* **7**, 4292.